ISSN 0001-4338, Izvestiya, Atmospheric and Oceanic Physics, 2018, Vol. 54, No. 4, pp. 336–343. © Pleiades Publishing, Ltd., 2018.
Original Russian Text © A.F. Kurbatskii, L.I. Kurbatskaya, 2018, published in Izvestiya Rossiiskoi Akademii Nauk, Fizika Atmosfery i Okeana, 2018, Vol. 54, No. 4, pp. 396–404.

Study of the Neutral Ekman Flow Using an Algebraic Reynolds Stress Model

A. F. Kurbatskii[a, *] and L. I. Kurbatskaya[b, **]

[a] *Khristianovich Institute of Theoretical and Applied Mechanics, Siberian Branch, Russian Academy of Sciences, Novosibirsk, 630090 Russia*

[b] *Institute of Computational Mathematics and Mathematical Geophysics, Siberian Branch, Russian Academy of Sciences, Novosibirsk, 630090 Russia*

**e-mail: kurbat@itam.nsc.ru*

***e-mail: L.Kurbatskaya@ommgp.sscc.ru*

Received September 28, 2017; in final form, November 2, 2017

Abstract—A recently developed fully explicit algebraic model of Reynolds stress and turbulent heat flux in a thermally stratified planetary atmospheric boundary layer without stratification has been used for a numerical study of the Ekman turbulent boundary layer over a homogeneous rough surface for different dimensionless surface Rossby numbers. A comparative analysis has been conducted for a closure model of the transport term in the prognostic equation of turbulent kinetic energy dissipation including third-order moments. Dependences of the total wind rotation angle on the Rossby number have been obtained. The calculated vertical profiles of mean velocity, turbulent stress, turbulent kinetic energy, surface-friction velocity, and boundary-layer height agree satisfactorily with observational and earlier obtained LES data.

Keywords: turbulent kinetic energy, transport term model, Ekman flow, numerical modeling

DOI: 10.1134/S0001433818040266

INTRODUCTION

Turbulence modeling remains a key topic in the atmospheric sciences to describe the significant turbulent transfer of heat and momentum in the atmospheric boundary layer [1]. Atmospheric boundary layer (ABL) studies are of great importance for solving weather-forecast problems and future scenarios of climate change in climatological models. It remains important to accurately reproduce the turbulent fluxes of momentum, heat, and moisture from the underlying surface with time varying temperature regime.

Many turbulence models used in climate simulations or weather forecasts are based on the concept of eddy viscosity. This model is inadequate for describing turbulent flows specifically because it fails to correctly specify the Reynolds stress anisotropy $\overline{u_i u_j}$. A more general approximation of the well-known hierarchy of turbulence models for geophysical turbulent flows [2] is based on transport equations for Reynolds stress $\overline{u_i u_j}$ and the vector of turbulent heat flux $\overline{u_i \theta}$. The use of an equation for the variance of temperature fluctuations (turbulent potential energy), coupled with an equation for the rate of dissipation of turbulent kinetic energy (TKE), makes it possible to take into account the nonlocal effect of turbulent heat transfer and correctly simulate the ABL dynamics in inversion layers. More significant progress has been made recently in developing more general (than the standard hypotheses on turbulent viscosity) models for eddy diffusivities of momentum and heat due to the use of differential equations for Reynolds stress and turbulent heat flux in the weakly equilibrium approximation [3–5], which disregards the advection and diffusion of some dimensionless quantities. For turbulent flows with buoyancy, i.e., temperature (density) as an active scalar, the mathematical derivation of the model becomes complicated due to the coupling between the Reynolds stress and heat flux caused by buoyancy terms. In the weakly equilibrium approximation, the coupled system of algebraic equations for turbulent momentum and scalar fluxes for the ABL can be solved analytically using the mathematical operation of symbolic algebra to obtain explicit (noniterative) expressions for turbulent fluxes of momentum ($\overline{u_i u_j}$) and heat ($\overline{u_i \theta}$).

In this paper we use an explicit algebraic model of turbulent momentum and heat fluxes for a stratified ABL [4, 5] to study the neutral Ekman boundary layer. The numerical results are regarded as an input module for the subsequent study of the dynamics of a stable ABL over the surface with steady and nonsteady cooling rates.

2. EQUATION OF TURBULENT KINETIC ENERGY DISSIPATION

A prognostic equation for the spectral flow of turbulent kinetic energy (its dissipation rate ε) is the most complex component of the Reynolds-Averaged Navier–Stokes (RANS) approximation. Actually, the ε equation must be modeled phenomenologically [6] by analogy with the TKE equation. Here it is assumed that the generation of dissipation occurs with the TKE generation rate, while its destruction occurs with the TKE destruction rate, and this concept gives a rather adequate model. The prognostic equation of TKE dissipation can be somewhat justified physically by the spectral cascade of turbulence energy only for neutrally stratified turbulence [7].

The exact equation for the transfer of turbulent energy dissipation $\varepsilon = \nu\overline{(\partial u_i/\partial x_j)^2}$ can be obtained by standard Reynolds averaging of the Navier–Stokes equation

$$\begin{aligned}\frac{\partial \varepsilon}{\partial t} + U_i\frac{\partial \varepsilon}{\partial x_j} + \frac{\partial}{\partial x_j}\overline{\varepsilon' u_j} &= -2\nu\overline{\frac{\partial u_j}{\partial x_i}\frac{\partial u_j}{\partial x_k}}\frac{\partial U_i}{\partial x_k} \\ &- 2\nu\overline{\frac{\partial u_i}{\partial x_j}\frac{\partial u_k}{\partial x_j}}\frac{\partial U_i}{\partial x_k} - 2\nu\overline{\frac{\partial u_i}{\partial x_k}\frac{\partial u_i}{\partial x_m}\frac{\partial u_k}{\partial x_m}} \\ &- 2\nu u_k\overline{\frac{\partial u_i}{\partial x_j}}\frac{\partial^2 U_i}{\partial x_k \partial x_j} - 2\nu\frac{\partial}{\partial x_k}\overline{\frac{\partial p}{\partial x_m}\frac{\partial u_k}{\partial x_m}} \\ - \nu\frac{\partial}{\partial x_k}\overline{u_k\frac{\partial u_i}{\partial x_m}\frac{\partial u_i}{\partial x_m}} &- 2\nu^2\overline{\left(\frac{\partial^2 u_i}{\partial x_k \partial x_m}\right)^2} + \nu\nabla^2\varepsilon.\end{aligned} \quad (1)$$

2.1. Closure of Prognostic Dissipation Equation

The right-hand side of Eq. (1) for TKE dissipation E contains seven high-order correlations, which are controlled by quantities that are associated with the short-wave region of turbulent spectrum. By scaling the relative magnitude of these correlations with the help of the turbulent Reynolds number, $\mathrm{Re}_L = (\hat{u}L)/\nu$ allows Eq. (1) to be simplified [6]:

$$\begin{aligned}\frac{\partial \varepsilon}{\partial t} + U_j\frac{\partial \varepsilon}{\partial x_j} + \frac{\partial}{\partial x_j}\overline{\varepsilon' u_j} \\ = -2\nu\overline{\frac{\partial u_i}{\partial x_k}\frac{\partial u_i}{\partial x_j}\frac{\partial u_j}{\partial x_k}} - 2\nu^2\overline{\left(\frac{\partial^2 u_i}{\partial x_j \partial x_k}\right)^2}.\end{aligned} \quad (2)$$

To obtain the closure of Eq. (2), one should formalize the transport term (the third term in the left-hand side) for the right-hand side of the equation as well.

The right-hand side of Eq. (2) describes the imbalance between the generation due to vorticity expansion and the dissipation destruction by viscosity. The right-hand side was proposed to be simulated using an approach [8] that is based on a polynomial representation of the right-hand side: the right-hand side is $= -\left(\varepsilon^2/E\right)\Psi$, where Ψ is a dimensionless function of invariants (Reynolds stress, turbulent heat flux, average velocity gradient, buoyancy, dissipation, and viscosity). The simplified expressions for Ψ can be found in [9, 10].

The transport term in Eq. (2) is normally assumed to be subjected to gradient diffusion. In the stationary horizontally homogeneous case, we have

$$\frac{\partial}{\partial z}\overline{\varepsilon' w} = -\frac{\partial}{\partial z}\left(\frac{K_m}{\sigma_\varepsilon}\frac{\partial \varepsilon}{\partial z}\right), \quad (3)$$

where K_m is the eddy diffusivity of momentum and σ_ε is the Schmidt number for the TKE dissipation rate.

This parameterization has no firm physical grounds. The nonlocal process of turbulent diffusion described by third-order moments is parameterized by the local model. The attractive simplicity of gradient diffusion model (3) for the transport term leads to difficulties in finding the turbulent Schmidt number σ_ε in the minimized (in terms of complexity and completeness) explicit algebraic Reynolds stress model, as is shown in Section 3 and from the results of a numerical simulation of the turbulent Ekman flow in Section 4.

The equations of the explicit algebraic model of Reynolds stress and turbulent heat flux for a thermally stratified ABL are given in the Appendix.

3. EXPLICIT ALGEBRAIC REYNOLDS MODEL IN THE NEUTRAL ATMOSPHERIC BOUNDARY LAYER

The ABL changes in time and space. Its structure depends on the Earth's rotation, horizontal pressure gradient and horizontal temperature gradient (baroclinicity), heat and moisture fluxes on the surface, virtual potential temperature stratification, turbulence intensity, and cloudiness, as well as the roughness, slope, and heterogeneity of the underlying surface.

A neutral ABL appears at a constant virtual potential temperature without heat and moisture fluxes on the surface and horizontal gradients of temperature and cloudiness. A neutral ABL has no buoyancy effects caused by heating or cooling the underlying surface. A neutrally stratified ABL is also often called an Ekman turbulent boundary layer (EBL).

Although the EBL is relatively rarely observed in field conditions, it is important to understand and quantitatively describe its turbulent structure for both the ABL theory and practical applications. One should know the turbulence structure to construct adequate turbulent closures used in global and mesoscale atmospheric circulation models.

The fully explicit (noniterative) algebraic model of Reynolds stress and turbulent heat flux of a thermally stratified ABL (Eqs. (A.1)–(A.6) in the Appen-

dix) is transformed for a neutral ABL to a simpler form of EBL:

$$\frac{DU}{Dt} = -\frac{\partial \overline{uw}}{\partial z} - f\left(V_g - V\right), \tag{4}$$

$$\frac{DV}{Dt} = -\frac{\partial \overline{vw}}{\partial z} + f\left(U_g - U\right), \tag{5}$$

$$\left(\overline{uw}, \overline{vw}\right) = -K_{m1}\left(\frac{\partial U}{\partial z}, \frac{\partial V}{\partial z}\right),$$

$$K_{m1} = \frac{1}{D_1}\frac{2}{3}\Delta_2 \frac{E^2}{\varepsilon} = C_{m1}\left(E^2/\varepsilon\right), \tag{6}$$

$$D_1 = 1 + d_1 G_M$$

$$= 1 + \frac{2}{3}\Delta_2^2\left[\frac{E}{\varepsilon}\right]^2\left[\left(\frac{\partial U}{\partial z}\right)^2 + \left(\frac{\partial V}{\partial z}\right)^2\right], \tag{7}$$

$$C_{m1} = \frac{(2/3)\Delta_2}{1 + (2/3)\Delta_2^2 (E/\varepsilon)^2\left[(\partial U/\partial z)^2 + (\partial V/\partial z)^2\right]}. \tag{8}$$

$\Delta_2 = (1 - C_2)/C_1 = 0.25$, where $C_1 = 2.0$ and $C_2 = 0.5$ are calibrated reference constants of the full turbulence model [4, 5].

$$\frac{DE}{Dt} = -\overline{uw}\frac{\partial U}{\partial z} - \overline{vw}\frac{\partial V}{\partial z} - \varepsilon + \frac{\partial}{\partial z}\left(\frac{K_{m1}}{\sigma_E}\frac{\partial E}{\partial z}\right), \tag{9}$$

$$\frac{D\varepsilon}{Dt} = -\frac{1}{2}\psi_0 \frac{\varepsilon^2}{E} + \frac{1}{2}\psi_1 \frac{\varepsilon}{E_k} P + \frac{\partial}{\partial z}\left(\frac{K_{m1}}{\sigma_\varepsilon}\frac{\partial \varepsilon}{\partial z}\right). \tag{10}$$

For the neutrally stratified case in the TKE balance equation

$$\partial E/\partial t = P - \varepsilon + D_E,$$

the transport term D_E in the near-surface sublayer of the surface is negligibly small and the TKE generation by a velocity shift is equal to the viscous dissipation:

$$-\overline{uw}\frac{\partial U}{\partial z} - \overline{vw}\frac{\partial V}{\partial z} = \varepsilon. \tag{11}$$

For the surface neutral sublayer, approximation (11) allows dissipation equation (10) to be written as

$$\frac{1}{2}(\psi_1 - \psi_0)\frac{\varepsilon^2}{E} = \frac{\partial}{\partial z}\left(\frac{C_{m1}}{\sigma_\varepsilon}\frac{E^2}{\varepsilon}\frac{\partial \varepsilon}{\partial z}\right). \tag{12}$$

To estimate the coefficient C_{m1} in (12), one can take into account (6) and (11) to derive from (8) the quadratic equation

$$C_{m1} = \frac{(2/3)\Delta_2}{1 + (2/3)\Delta_2^2\left[\left(E/u_*^2\right)^2 C_{m1}^2\right]^{-1}}, \tag{13}$$

where the numerical value of E/u_*^2 should be determined. Using (for simplicity) the standard model of eddy viscosity with the constant coefficient $C_{m1} = 0.09$ [11] in (6), we obtain from (6) and (11) in the surface neutral sublayer of the surface layer

$$E = \frac{u_*^2}{\sqrt{C_{m1}}} = \frac{10}{3}u_*^2, \tag{14}$$

where u_* is the friction velocity on the surface. Quadratic equation (13) with (14) and $\Delta_2 = 0.25$ has the roots $C_{m1}^{(1)} = 0.14$ and $C_{m1}^{(2)} = 0.028$. According to (12), the first root $C_{m1}^{(1)}$ with the Karman constant $k = 0.4$ yields the turbulent Schmidt number

$$\sigma_\varepsilon = (10/3)^3 \frac{C_{m1}k^2}{(\psi_1 - \psi_0)/2} = 1.18. \tag{15}$$

The second root $C_{m1}^{(2)}$ leads to a too small turbulent Schmidt number ($\sigma_\varepsilon = 0.23$). The resulting value $\sigma_\varepsilon = 1.18$ is close to $\sigma_\varepsilon = 1.3$ obtained in [11] and adopted in [12]. In the standard E–ε model, the coefficient C_{m1} is assumed to be constant (0.09 in engineering applications [11] or 0.033 in the atmospheric context [13]); however, the coefficient C_{m1} in the present explicit algebraic Reynolds stresses model varies according to (8) in altitude with the change in turbulence scale $\tau = E/\varepsilon$ and vertical gradients of the average wind-velocity components.

According to numerical results, the model correctly reproduces all the main ABL characteristics; however, the use of the turbulent Schmidt number $\sigma_\varepsilon = 1.18$ in the ε equation results in overestimated vertical distributions of TKE and eddy diffusivity of momentum.

According to the LES calculation results [14], for a neutral ABL the shear generation and viscous dissipation in the E equation up to heights $\sim 0.3u_*/f$ are an order of magnitude higher than the transport term, which further takes an increasing value. Since the transport term in the ε equation acts as a source term in local processes, the turbulent diffusion of dissipation should be increased by decreasing the turbulent Schmidt number σ_ε. The value of σ_ε can be found by comparing the calculated EBL characteristics with the results of other RANS and LES calculations (see Section 4.2). The turbulent Schmidt number was found by numerical optimization to be $\sigma_\varepsilon = 0.65$.

The explicit algebraic model of the Reynolds stress and turbulent heat flux [12] uses the value $\sigma_\varepsilon = 1.3$, similar to engineering applications [11]. Unlike the present explicit algebraic model of Reynolds stress, the model described in [12] had no limiting case for a neutral ABL and was verified directly in a stable ABL.

The turbulent Schmidt number σ_E in TKE balance equation (9) is fixed to be unity similar to other three- and two-parameter turbulence models [12, 13].

4. NUMERICAL SIMULATION: ESTIMATE FOR THE SENSITIVITY OF THE MODEL OF THE TRANSPORT TERM IN THE ε EQUATION TO THE TURBULENT SCHMIDT NUMBER σ_ε

In this numerical study, the profile of initial velocity is taken to be uniform in height and equal to the geostrophic wind velocity: $U = G = 8$ m/s, $V = 0$. The structure of a neutral ABL is controlled only by one dimensionless parameter—the surface Rossby number $\mathrm{Ro} = U_g/(fz_0)$, which gives the geostrophic friction coefficient $C_g = u_*/G$ [15]. The value of the Coriolis parameter $f = 10^{-4}$ s^{-1} was taken for moderate latitudes ($\varphi = 52.5°$). The neutral boundary layer specifies its proper thickness [16], which is multiple to $h = u_*/f$; the height h should exceed this "natural" thickness to have no influence on the boundary layer structure. In the numerical integration, the value of h is chosen so that the neutral structure of the boundary layer remains unchanged below h.

When specifying the initial distribution of TKE $E_0 = 3.75u_*^2 z_1/z$ and its dissipation rate $\varepsilon_1 = u_*^3/(kz)$ $(z \geq z_1)$, the friction velocity u_* was determined by the geostrophic coefficient $C_g = u_*/G$ over the fixed Rossby number according to [17].

We assume that the existence of a logarithmic layer with the magnitude of mean horizontal velocity is justified:

$$|\mathbf{U}|/u_* = k^{-1}\ln(z/z_0). \tag{16}$$

Here, it makes sense to note the validity of logarithmic law (16) for heights $z > 10z_0$ [18]. For heights below the level $10\,z_0$, the ABL is affected by local pressure forces caused by roughness elements. Therefore, it is not quite justified to specify boundary values at $z = z_0$ (like, for example, in the E–ε–$\overline{\theta^2}$-model [12]).

The friction velocity is calculated analytically from the logarithmic law for magnitude of mean wind velocity (16)

$$u_* = k\frac{\sqrt{U(z_2)^2 + V(z_2)^2}}{\ln(z_2/z_0)}. \tag{17}$$

At the upper boundary of the computational domain ($z = h$), we have

$$\frac{\partial U}{\partial z} = \frac{\partial V}{\partial z} = \frac{\partial E}{\partial z} = \frac{\partial \varepsilon}{\partial z} = 0. \tag{18}$$

At the lower boundary, in the first node of the difference grid ($z = z_1$; $z_1 > 10z_0$), we have

$$E_1 = 3.75u_*^2, \quad \varepsilon_1 = u_*^3/kz_1, \tag{19}$$

according to the measurement data presented in [10].

Assuming that the effect of the Coriolis forces in the surface layer is small and taking into account (16), one can ensure that in the first two nodes of the difference grid the following condition is satisfied:

$$\frac{U(z_1)}{U(z_2)} = \frac{V(z_1)}{V(z_2)} = \frac{\ln(z_1/z_0)}{\ln(z_2/z_0)}, \tag{20}$$

which is used as a boundary condition for wind velocity components.

The calculated values of the main characteristics of a neutral EBL are shown in Figs. 1–4. System of equations (4)–(10) for given initial and boundary conditions was solved using a semi-implicit finite-difference scheme [19] on a staggered grid with a time step of 2.5 s and a vertical coordinate of 3.125 m.

4.1. Velocity Profiles, the Ekman Spiral, Friction Velocity, and Logarithmic Profile of Wind Speed

Figure 1a shows the profiles of mean wind velocity components $U(z)$ and $V(z)$ for two Rossby numbers. Figure 1b shows the Ekman spiral for mean wind velocity. Unlike the classical Ekman spiral with a constant (by height) viscosity coefficient and a wind rotation angle of 45°, the Ekman spirals in a turbulent Ekman boundary layer with a variable (by height) eddy diffusivity are located considerably closer to the geostrophic wind direction. The most variable parameter in determining the Rossby number is the surface roughness height z_0. For a larger Rossby number (smaller value of z_0), the Ekman spiral fixes a smaller wind rotation angle: $\alpha = 15.4°$ ($\mathrm{Ro} = 8 \times 10^6$, $z_0 = 0.01$ m) and $\alpha = 18.4°$ ($\mathrm{Ro} = 8 \times 10^5$, $z_0 = 0.1$ m). These values of the total angle of mean wind rotation are consistent with the data presented in [17, 21].

The logarithmic profile of velocity in the surface layer is determined by friction velocity. Figure 2a shows the calculated magnitude of velocity $M(z) = \left[U^2(z) + V^2(z)\right]^{1/2}$ in a semilogarithmic scale. The logarithmic profile is reproduced by the model well. The plot slope near the surface depends on friction velocity. The straight line stands for the theoretical logarithmic profile $M(z) = (u_*/k)\ln(z/z_0)$. Figure 2b shows the friction velocity on the surface as a function of the integration time. The friction velocity on the surface $u_* = C_g G$ decreases with increasing Rossby number, like in LES calculations [20]. In the steady state of the boundary layer (Fig. 2b), we have $u_* = 0.28$ m/s ($\mathrm{Ro} = 8 \times 10^5$) for the friction velocity on the surface; $C_g = (u_*/G) \cong 0.035$) for the geostrophic friction coefficient; and $u_* = 0.24$ m/s ($\mathrm{Ro} = 8 \times 10^6$), $C_g = (u_*/G) \cong 0.03$ for friction velocity.

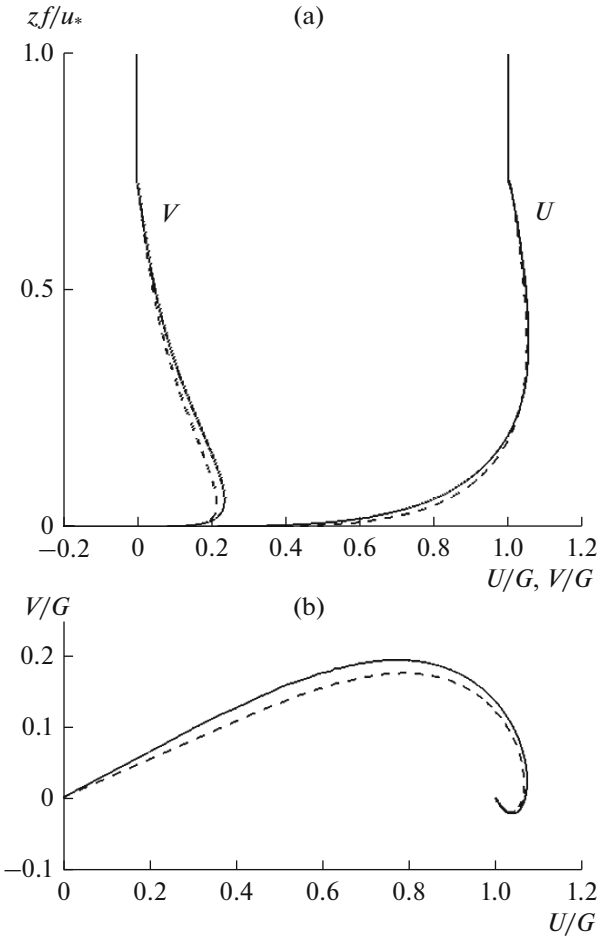

Fig. 1. Profiles of wind-velocity components (a) and the Ekman spiral of mean wind velocity (b) for two Rossby numbers Ro (the dimensionless height zf/u_* is along the vertical axis and the dimensionless velocity components are along the horizontal axis, $G = 8$ m/s, the solid line is $z_0 = 0.1$ m, and the dashed line is $z_0 = 0.01$ m).

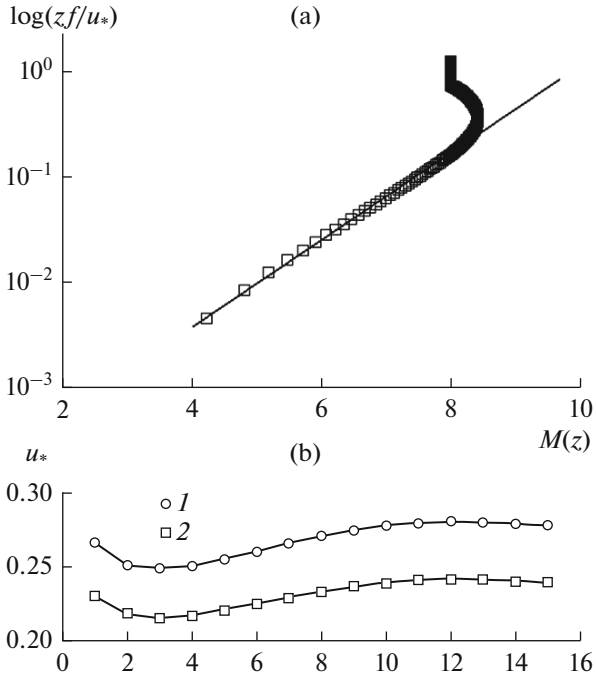

Fig. 2. (a) Logarithmic profile of velocity in the surface layer for $\mathrm{Ro} = 8 \times 10^5$ (the squares denote the real profile, the straight line denotes the logarithmic profile, the logarithm of dimensionless height is along the vertical axis, and the wind magnitude of wind velocity $M(z)$ in m/s is along the horizontal axis); (b) friction velocity on the surface u_* (m/s) as a function of time (in hours): $z_0 = 0.1$ m (curve *1*) and $z_0 = 0.01$ m (curve *2*).

4.2. Turbulent Stress Profiles, Turbulent Kinetic Energy, and Eddy Diffusivity of Momentum. Boundary Layer Height

The statistics of turbulence is shown in Fig. 3 by vertical profiles of the total turbulent stress $\tau = \sqrt{\left(-\overline{uw}\right)^2 + \left(-\overline{vw}\right)^2}$ and turbulent kinetic energy $E = \overline{u_i^2}/2$. For comparison, the profiles of total turbulent stress (subgrid and resolved) obtained from a LES calculation are presented [20]. In Fig. 3b, the solid and dashed-and-dotted lines correspond to the profile of TKE E/u_*^2 ($\sigma_\varepsilon = 0.65$) and the profile obtained from a LES calculation [20], respectively. The distributions of τ and TKE in the LES calculation do not imply that τ and TKE tend to zero with the growth of height (Figs. 3a, 3b). This seems to be caused by insufficient vertical resolution of the computational domain. For comparison, the profile obtained with $\sigma_\varepsilon = 1.18$ (dashed line) is shown. For this turbulent Schmidt number, the vertical distribution of TKE turns out to be overestimated starting from the height $0.2zf/u_*$. The overestimated value of TKE leads to an overestimated distribution of eddy diffusivity of momentum (the dashed line in Fig. 4a). Figure 4a shows the vertical profiles of eddy diffusivity of momentum $K_m f/u_*^2$ calculated by an explicit algebraic Reynolds stress model in comparison with the results obtained by other authors. The solid line marked with black dots and the dashed line corresponds to the values calculated with turbulent Schmidt numbers $\sigma_\varepsilon = 0.65$ and $\sigma_\varepsilon = 1.18$. In the neutral ABL, this clearly indicates the influence of the turbulent Schmidt number in the ε equation: the maximum value of $K_m f/u_*^2$ at $\sigma_\varepsilon > 1$ ($\sigma_\varepsilon = 1.18$) significantly exceeds that value at $\sigma_\varepsilon = 0.65$, when the behavior of eddy diffusivity of momentum is consistent with other results. The solid line (marked with black squares) indicates the eddy diffusivity of momentum obtained by numerical simulation [10] using prognostic equations for Reynolds

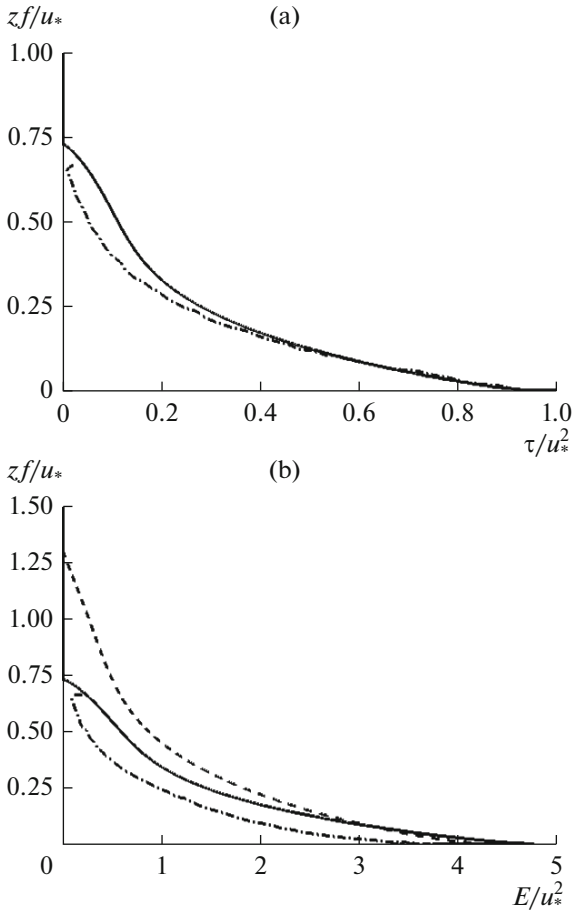

Fig. 3. (a) Profiles of turbulent stress $\tau = \sqrt{\left(-\overline{uw}\right)^2 + \left(-\overline{vw}\right)^2}$: solid line ($\sigma_\varepsilon = 0.65$), dashed-and-dotted line (LES calculation [20]), and the dimensionless height zf/u_* is along the vertical axis; (b) TKE profiles: solid line ($\sigma_\varepsilon = 0.65$), dashed line ($\sigma_\varepsilon = 1.18$), and dashed-and-dotted line (LES calculation [20]). The quantities of TKE and stress are made dimensionless to u_*^2, and all the profiles are given for the case $z_0 = 0.1$ m).

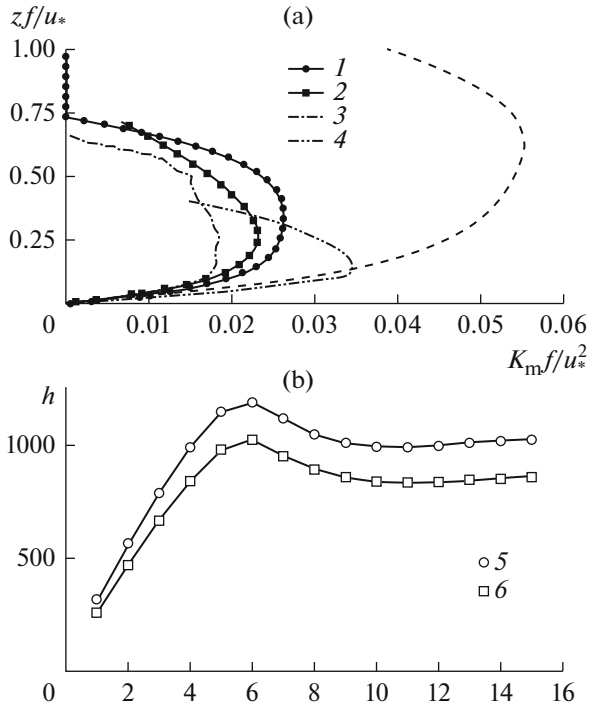

Fig. 4. (a) Profiles of eddy diffusivity of momentum: solid line *1* ($\sigma_\varepsilon = 0.65$), dashed line ($\sigma_\varepsilon = 1.18$), solid line *2* (RANS calculation [10]), dashed-and-dotted line *3* (LES calculation [20]), and dashed-and-dotted line *4* (laboratory experiment [23]); (b) boundary layer height h (m): curve *5* ($z_0 = 0.1$ m) and curve *6* ($z_0 = 0.01$ m). The horizontal axis shows the time in hours.

stress, the dashed-and-dotted line indicates the results obtained from a LES calculation [20], and the dashed-and-dotted line with two points indicates experimental data [23].

The boundary-layer height was determined from the condition that the turbulent stress at this height is 5% of the surface stress. Figure 4b shows the time dependence of boundary layer height for two different Rossby numbers. At the initial stage of integration with the boundary layer evolution, its height increases and the growth rate decreases with increasing Rossby number. In 10 h, the evolution process is terminated and the boundary layer height reaches a steady state. The change in the boundary layer height has the same character in the LES calculation [20]. Comparing the characteristic vertical scale u_*/f of the neutral ABL with the calculated boundary layer height h, one can find the dimensionless boundary layer height (the so-called Rossby–Montgomery constant $C_R = hf/u_*$). Its values are 0.36 (for $z_0 = 0.1$) and 0.35 (for $z_0 = 0.01$). This constant under real conditions does not exceed 0.2–0.3. The difference is due to the fact that the models consider a purely neutral boundary layer in a neutrally stratified atmosphere. A fully neutral boundary layer in the real atmosphere is rarely observed. For example, the measurements [22] in the EBL over the water surface were made under only approximately neutral and barotropic conditions. The boundary layer height was $\cong 0.2u_*/f$ because of a weakly stable layer at the top: the measured vertical profile of potential temperature was neutral up to a certain height and had a stable gradient at the top.

5. CONCLUSIONS

A numerical simulation of a neutrally stratified ABL has been performed. This is a classical problem in geophysical hydromechanics. The novelty of this study is in the use of an explicit algebraic model for turbulent momentum fluxes, which is a limiting case of the full explicit model of turbulent momentum and heat fluxes

for a thermally stratified ABL. The model correctly reproduces the vertical profiles of mean wind velocity, the tangential turbulent stress, the vertical distribution of TKE, and the behavior of the Ekman spiral of the mean wind as a function of the Rossby number. The resulting characteristics of the neutral turbulent Ekman flow are supposed to be used as input data for a numerical study of the evolution of the structure of a stably stratified planetary boundary layer with an unsteady surface cooling rate.

APPENDIX

Explicit Algebraic Model of Reynolds Stress and Turbulent Heat Flux for the Planetary Boundary Layer

The fully explicit algebraic model for turbulent momentum and heat fluxes for a planetary ABL has the form [4, 5]

$$\frac{DE}{Dt} = -\overline{uw}\frac{\partial U}{\partial z} - \overline{vw}\frac{\partial V}{\partial z} + \frac{g}{T_0}\overline{w\theta} - \varepsilon + \frac{\partial}{\partial z}\left(\frac{K_m}{\sigma_E}\frac{\partial E}{\partial z}\right), \quad (A.1)$$

$$\frac{D\varepsilon}{Dt} = -\frac{1}{2}\psi_0\frac{\varepsilon^2}{E} + \frac{1}{2}\psi_1\frac{\varepsilon}{E}(P+G) + \psi_2\frac{g}{T_0}\left(\overline{u\theta}\frac{\partial U}{\partial z} + \overline{v\theta}\frac{\partial V}{\partial z}\right) + \frac{\partial}{\partial z}\left(\frac{K_m}{\sigma_\varepsilon}\frac{\partial \varepsilon}{\partial z}\right), \quad (A.2)$$

$$\frac{D\overline{\theta^2}}{Dt} = -2\overline{w\theta}\frac{\partial \Theta}{\partial z} - \frac{1}{r}\frac{\varepsilon}{E}\overline{\theta^2} + \frac{\partial}{\partial z}\left(\frac{K_m}{\sigma_{\overline{\theta^2}}}\frac{\partial \overline{\theta^2}}{\partial z}\right). \quad (A.3)$$

$$\left(\overline{uw}, \overline{vw}\right) = -K_m\left(\frac{\partial U}{\partial z}, \frac{\partial V}{\partial z}\right), \quad \overline{w\theta} = -K_h\frac{\partial \Theta}{\partial z} + \gamma_c, \quad (A.4)$$

$$\gamma_c = \frac{1}{D}\left[1 + \frac{2}{3}\Delta_2^2 G_M + \lambda_1\Delta_3 G_H\right]\lambda_2(\tau\alpha g)\overline{\theta^2}.$$

$$D = 1 + d_1 G_M + d_2 G_H + d_3 G_H^2 - d_4 G_M G_H,$$

$$d_1 = \frac{2}{3}\Delta_2^2; \quad d_2 = \frac{7}{3}\lambda_1\Delta_3; \quad d_3 = \frac{4}{3}(\lambda_1\Delta_3)^2;$$

$$d_4 = \frac{2}{3}\lambda_1\lambda_2\Delta_2\Delta_3.$$

$$G_M = (\tau S)^2, \quad G_H = (\tau N)^2, \quad N^2 = \alpha g\frac{\partial \Theta}{\partial z},$$

$$S^2 = \left(\frac{\partial U}{\partial z}\right)^2 + \left(\frac{\partial V}{\partial z}\right)^2.$$

$$K_m = \frac{1}{D}\left[\frac{2}{3}\Delta_2 E\tau\left(1 - \frac{\Delta_3}{\Delta_2}\lambda_1\lambda_2 G_H\right) + \lambda_2\Delta_3\left(\lambda_2 + \frac{4}{3}\Delta_2\right)\tau(\tau\alpha g)^2\overline{\theta^2}\right], \quad (A.5)$$

$$K_h = \frac{1}{D}\left[\frac{2}{3}\lambda_1 E\tau(1 + \lambda_1\Delta_3 G_H)\right], \quad (A.6)$$

$$\Delta_1 = \frac{4}{3}\frac{(1-C_2)}{C_1}, \quad \Delta_2 = \frac{(1-C_2)}{C_1}, \quad \Delta_3 = \frac{(1-C_3)}{C_1},$$

$$\lambda_1 = 1/C_{1\theta}, \quad \lambda_2 = \frac{(1-C_{2\theta})}{C_{1\theta}}.$$

The calibrated base constants of the model are $C_1 = 2.0$; $C_2 = 0.5$; $C_3 = 0.5$; $C_{1\theta} = 3.28$; $C_{2\theta} = 0.5$; $r = 0.6$.

The countergradient term γ_c in the turbulent heat flux $\overline{w\theta}$ takes into account the contribution of large-scale eddies in the vertical heat transfer.

The right-hand side of Eq. (A.2) is written in a form that is suitable for neutral, stable, and convective cases with calibrated constant parameters $\psi_0 = 3.8$, $\psi_1 = 2.4$, and $\psi_2 = 0.3$ [9]. P and G denote the generation by shear and buoyancy, respectively, like in TKE balance equation (A.1). The right-hand side of Eq. (A.2) in a somewhat different form was used in [12].

ACKNOWLEDGMENTS

This study was supported in part by the Russian Foundation for Basic Research, project no. 17-01-00137.

REFERENCES

1. A. A. M. Holtslag, G. Svensson, P. Baas, S. Basu, B. Beare, A. C. M. Beljaars, F. C. Bosveld, J. Cuxart, J. Lindvall, G. J. Steeneveld, M. Tjernström, and B. J. H. Van deWiel, "Stable atmospheric boundary layers and diurnal cycles: Challenges for weather and climate models," Bull. Am. Meteorol. Soc. **94** (11), 1691–1706 (2013).
2. G. L. Mellor and T. Yamada, "Development of a turbulence closure model for geophysical fluid problems," Rev. Geophys. Space Phys. **20** (4), 851–875 (1982).
3. Y. Cheng, V. M. Canuto, and A. M. Howard, "An improved model for the turbulent PBL," J. Atmos. Sci. **59** (5), 1550–1565 (2002).
4. A. F. Kurbatskii and L. I. Kurbatskaya, "Three-parameter model of turbulence for the atmospheric boundary layer over an urbanized surface," Izv., Atmos. Ocean. Phys. **42** (4), 439–455 (2006).
5. A. F. Kurbatskii and L. I. Kurbatskaya, "$E - \varepsilon - \overline{\theta^2}$ turbulence closure model for an atmospheric boundary layer including the urban canopy," Meteorol. Atmos. Phys. **104** (1–2), 63–81 (2009).
6. Tennekes, H. and Lumley, J.L., *A First Course in Turbulence* (MIT, Cambridge, 1972).
7. J. Lumley, "Fundamental aspects of incompressible and compressible turbulent flows," in *Simulation and Modelling of Turbulent Flows*, Ed. by T. B. Gatski, M. Y. Hussaini, and J. L. Lumley (Oxford University Press, New York, 1996), pp. 5–78.
8. J. L. Lumley, "Computational modeling of turbulent flows," in *Advances in Applied Mechanics*, Ed. by C. S. Yih (Academic, New York, 1978), Vol. 18, pp. 123–176.

9. A. Andren, "A TKE-dissipation model for the atmospheric boundary layer," Boundary Layer Meteorol. **56** (3), 207–221 (1991).
10. J. C. Wyngaard, O. R. Coté, and K. S. Rao, "Modeling the atmospheric boundary layer," Adv. Geophys. **18A**, 193–211 (1975).
11. D. E. Launder and D. B. Spalding, "The numerical computation of turbulent flows," Comput. Methods Appl. Mech. Eng. **3** (2), 269–289 (1974).
12. W. M. J. Lazeroms, G. Svensson, E. Bazile, G. Brethouwer, S. Wallin, A. V. Johansson, "Study of transitions in the atmospheric boundary layer using explicit algebraic turbulence models," Boundary-Layer Meteorol. **161** (1), 19–47 (2016).
13. P. G. Duynkerke, "Application of the turbulence closure model to the neutral and stable atmospheric boundary layer," J. Atmos. Sci. **45** (5), 865–880 (1988).
14. P. J. Mason and D. J. Thomson, "Large-eddy simulation of the neutral-static-stability planetary boundary layer," Q. J. R. Meteorol. Soc. **113**, 413–443 (1987).
15. S. S. Zilitinkevich, "Velocity profiles, resistance laws and dissipation rate of mean flow kinetic energy in a neutrally and stably stratified planetary boundary layer," Boundary-Layer Meteorol. **46** (4), 367–387 (1989).
16. A. K. Blackadar and H. Tennekes, "Asymptotic similarity in neutral barotropic planetary boundary layers," J. Atmos. Sci. **25** (6), 1015–1020 (1968).
17. S. S. Zilitinkevich, *The Dynamics of the Atmospheric Boundary Layer* (Gidrometeoizdat, Leningrad, 1970) [in Russian].
18. J. Lumley and H. Panofsky, *The Structure of Atmospheric Turbulence* (Interscience Publishers, New York, 1964; Mir, Moscow, 1966).
19. P. Roache, Computational Fluid Dynamics (Hermosa, Albuquerque, N.M., 1972; Mir, Moscow, 1980).
20. M. V. Shokurov, S. Yu. Artamonov, and I. N. Ezau, "Numerical modeling of a neutrally stratified atmospheric boundary layer," Morsk. Gidrofiz. Zh., No. 2, 37–50 (2013).
21. A. K. Blackadar, "The vertical distribution of wind and turbulent exchange in a neutral atmosphere," J. Geophys. Res. **67** (8), 3095–3102 (1962).
22. S. Nicholls, "Aircraft observations of the Ekman layer during the joint air–sea interaction experiment," Q. J. R. Meteorol. Soc. **111**, 391–426 (1985).
23. J. Q. Hinze, *Turbulence* (McGraw-Hill, New York, 1975).

Translated by V. Arutyunyan